A $\delta^{34}S_{SO_4}$ approach to reconstructing biogenic pyrite burial in carbonate-evaporite basins: An example from the Ara Group, Sultanate of Oman

D.A. Fike* and J.P. Grotzinger
Division of Geological and Planetary Sciences, California Institute of Technology, Pasadena, California 91125, USA

ABSTRACT

Carbonate-associated sulfate (CAS) has the potential to generate high-resolution records of seawater sulfate ($\delta^{34}S_{SW}$) that improve upon existing evaporite-based records. With improved resolution, however, significant isotopic offsets have become apparent between the evaporite and CAS proxies. Here we present high-resolution $\delta^{34}S$ measurements of both these proxies from the Ara Group, Sultanate of Oman, a series of six carbonate-evaporite sequences deposited ca. 547–540 Ma. The $\delta^{34}S_{CAS}$ from Ara carbonates show little scatter and provide our estimate of $\delta^{34}S_{SW}$. Repeated enrichments (as much as 4‰ relative to $\delta^{34}S_{CAS}$) were observed in floor and roof anhydrite units ($\delta^{34}S_{EVAP}$) bounding the Ara carbonates. These enrichments cannot be explained by secular variation or from isotopic fractionation during evaporite deposition and require the existence of an additional ^{34}S-depleted sink, which we attribute to H_2S production via ongoing bacterial sulfate reduction during evaporite deposition. To preserve this isotope signature, the resulting sulfide must be sequestered as pyrite. The magnitude of the resulting $\delta^{34}S_{EVAP}$ offset (relative to CAS) is a function of local pyrite burial (f_{pyr}). In periods of low pyrite burial, it is possible for $\delta^{34}S_{EVAP}$ to be depleted relative to $\delta^{34}S_{SW}$, whereas during episodes of substantial pyrite burial ($f_{pyr} > 0.05$), $\delta^{34}S_{EVAP}$ can be strongly enriched relative to $\delta^{34}S_{SW}$. Our data suggest that local f_{pyr} of ~0.13 is consistent with the observed $\delta^{34}S_{EVAP}$ enrichments found in the Ara Group anhydrites. Such elevated pyrite burial in evaporitic settings requires a substantial iron source, supporting possible ferruginous ocean conditions across the Ediacaran-Cambrian boundary. Isotopic offsets between paired $\delta^{34}S_{CAS}$-$\delta^{34}S_{anhydrite}$ data may thus serve as an independent proxy for marine redox through time, in addition to quantifying the importance of microbial activity in a setting where direct evidence (e.g., total organic carbon or biomarkers) may be scarce and physical processes are thought to dominate.

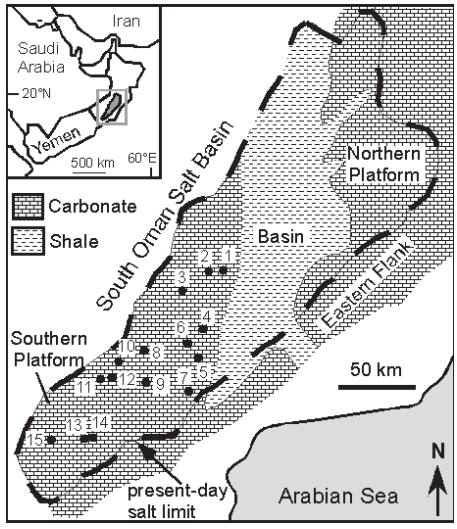

Figure 1. Map of Oman showing locations of wells from South Oman Salt Basin that provided subsurface samples. Well key: 1—BBN-2; 2—BBN-1; 3—MNH-1; 4—BRB-4; 5—BHR-1; 6—DRR-1; 7—NAQ-1; 8—RBB-3; 9—SAR-2; 10—ZAL-1; 11—ZAL-2; 12—ZAL-3; 13—GFR-4; 14—GFR-5; 15—QSB-1.

INTRODUCTION

The global sulfur cycle is one of the principal biogeochemical means to regulate Earth's surface redox over geologic time (Garrels and Lerman, 1981). Measurement of the sulfur isotopic composition of seawater sulfate [$\delta^{34}S_{SW} = (^{34}S/^{32}S)_{SW}/(^{34}S/^{32}S)_{STD} - 1 \times 10^3$, relative to the international Vienna Canyon Diablo Troilite standard] is one of the most useful tools for reconstructing ancient sulfur cycling. Studies have traditionally relied on sparsely distributed marine sulfate evaporites, which are believed to reasonably approximate $\delta^{34}S_{SW}$ (Claypool et al., 1980). Additional proxies, such as carbonate-associated sulfate (CAS) (Burdett et al., 1989), have the potential to provide a more complete $\delta^{34}S_{SW}$ record over Earth history (Fike et al., 2006; Kampschulte and Strauss, 2004). Although first-order trends in CAS and evaporite $\delta^{34}S$ are similar, significant offsets (>10‰) are observed between these proxies for $\delta^{34}S_{SW}$ throughout Phanerozoic strata (Kampschulte and Strauss, 2004). Although some of these differences may be attributed to secular $\delta^{34}S_{SO_4}$ variability between noncontemporaneous strata, this is unlikely to account for all of these offsets. In particular, in strata containing interbedded carbonate and evaporites (thereby eliminating errors due to correlation and secular variability), $\delta^{34}S_{EVAP}$ can be offset from $\delta^{34}S_{CAS}$ by as much as 5‰ (Kah et al., 2004).

It is the aim of this paper to investigate isotopic offsets between CAS ($\delta^{34}S_{CAS}$) and anhydrite ($\delta^{34}S_{EVAP}$) preserved in Ara Group strata from the Sultanate of Oman. The rapid deposition of carbonate-evaporite sequences precludes substantial secular variation in $\delta^{34}S_{SW}$. As such, offsets between $\delta^{34}S_{CAS}$ and $\delta^{34}S_{EVAP}$ can be used to probe local (e.g., basinal) paleoenvironmental conditions and marine chemistry at the time of their deposition.

GEOLOGICAL SETTING

The Ara Group is a series of six carbonate-evaporite cycles (Schröder et al., 2003) deposited between ca. 547 and 540 Ma (Bowring et al., 2007) in the South Oman Salt Basin, Sultanate of Oman (Fig. 1). The Ara Group encompasses the late Ediacaran–early Paleozoic $\delta^{34}S_{SW}$ maximum (Claypool et al., 1980) and contains ^{34}S-enriched anhydrite (Schröder et al., 2004) and CAS (Fike and Grotzinger, 2008).

Each Ara cycle can be divided into three phases: (1) deposition of a floor anhydrite during a period of freshening; (2) an open marine phase of carbonate platform development; and (3) deposition of a roof anhydrite, and ultimately halite, during a period of increasing basin restriction. The maximum flooding surface (MFS) is commonly located close to the anhydrite-carbonate transition (Schröder et al., 2003). This contact likely represents a dissolution surface (Fig. DR1 in the GSA Data Repository[1]) that formed as open marine waters entered the restricted basin. Depletions in $\delta^{13}C$ and $\delta^{34}S$ (CAS and anhydrite) are commonly observed at the MFS and likely reflect the oxidation during basin flooding of organic matter and sulfides, including H_2S, metastable FeS, and/or pyrite

*E-mail: dfike@levee.wustl.edu.
*Current address: Department of Earth and Planetary Sciences, and McDonnell Center for the Space Sciences, Washington University, St. Louis, Missouri 63130, USA

[1]GSA Data Repository item 2010094, methods and Figures DR1 and DR2, is available online at www.geosociety.org/pubs/ft2010.htm, or on request from editing@geosociety.org or Documents Secretary, GSA, P.O. Box 9140, Boulder, CO 80301, USA.

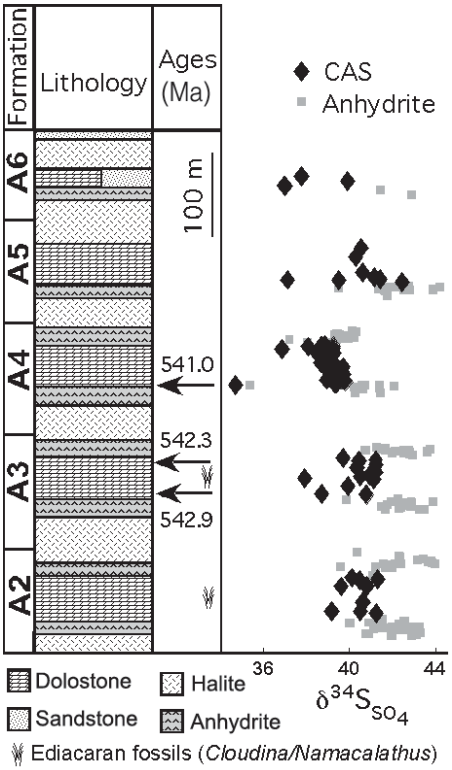

Figure 2. Composite stratigraphy of Ara Group units A2–A6. U/Pb ages are from Bowring et al. (2007). Samples from different wells are normalized to constant thickness for each carbonate and/or anhydrite unit for plotting purposes. Note enrichment in $\delta^{34}S_{EVAP}$ (evaporite; gray) relative to $\delta^{34}S_{CAS}$ (carbonate-associated sulfate; black). Depleted values at basal anhydrite-carbonate context are attributed to oxidation at maximum flooding surface. For data, see Table DR1 (see footnote 1).

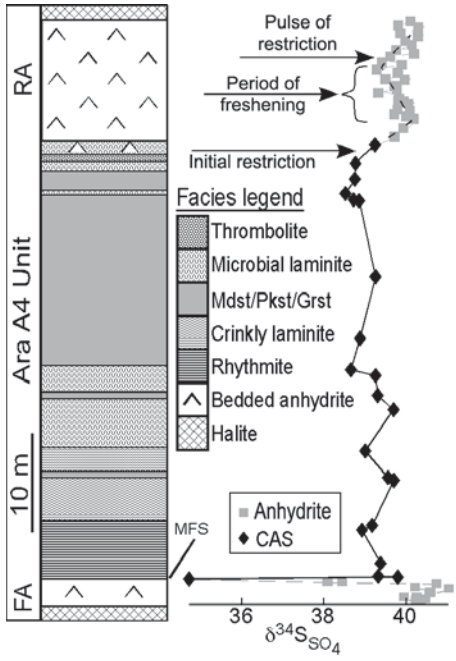

Figure 3. Variability in $\delta^{34}S$ over single carbonate-evaporite cycle (A4 cycle from well BRB-4 is shown). Carbonate facies were discussed in detail in Schröder et al. (2003) and are highlighted here to show facies independence of $\delta^{34}S_{CAS}$. Higher order changes in $\delta^{34}S_{EVAP}$ (evaporite) in roof anhydrite (RA) are interpreted to reflect pulses of restriction and freshening. Depleted $\delta^{34}S$ values (CAS, carbonate-associated sulfate, and anhydrite) found at contact between floor anhydrite (FA) and base of carbonate layer (maximum flooding surface) are attributed to oxidation associated with basin flooding. Mdst—mudstone; Pkst—packstone; Grst—grainstone.

(Figs. 2 and 3). The contacts between carbonate and overlying roof anhydrite are conformable (Amthor et al., 2002) and represent a shallowing-upward sequence where the uppermost meters of carbonate, deposited at or above wave base, are stromatolitic and interbedded with lenses of anhydrite (Schröder et al., 2003). Ara carbonates are preserved predominantly as dolomite (Schröder et al., 2003), and the anhydrites bounding the base and top of the Ara carbonates most likely were deposited as gypsum and underwent recrystallization to anhydrite during burial; however, this transformation is unlikely to have altered the original $\delta^{34}S$ composition (Worden et al., 1997). Fluid inclusion analysis (Brennan et al., 2004; Schröder et al., 2003) indicates that the evaporitic fluid was derived from seawater, precluding significant alteration by brines of nonmarine origin.

Ara Group strata are known definitively only from the subsurface. Anhydrite and carbonate samples analyzed in this study were collected from drill core and cuttings from multiple wells across the Ara basin (Fig. 1). Additional $\delta^{34}S_{CAS}$ data, previously reported from five wells (Fike and Grotzinger, 2008), are also shown. For a description of extraction and analytical methods, see the Data Repository.

RESULTS

High-resolution measurements of $\delta^{34}S_{EVAP}$ were obtained throughout the floor and roof anhydrites that bound Ara platform carbonates (Figs. 2 and 3). Note that the lowermost cycle A1 is excluded from discussion here, as it does not have a well-developed anhydrite-carbonate-anhydrite package. $\delta^{34}S_{CAS}$ showed little variation throughout the A2–A6 units documented here, except for an ~1‰ decrease over the A4 (Fig. 2). This pattern is also observed in nonevaporite carbonates from the Eastern Flank of the South Oman Salt Basin (Fike and Grotzinger, 2008). $\delta^{34}S_{CAS}$ is known to record $\delta^{34}S_{SW}$ in open marine conditions (Lyons et al., 2004) and the $\delta^{34}S_{CAS}$ trend in Ara strata has been interpreted to represent (global) secular change (Fike and Grotzinger, 2008).

Generally, $\delta^{34}S_{EVAP}$ follows the secular trend seen in $\delta^{34}S_{CAS}$. However, whereas $\delta^{34}S_{CAS}$ typically shows very little scatter (~1‰) within each carbonate unit, $\delta^{34}S_{EVAP}$ is more variable and typically enriched by as much as 4‰ relative to $\delta^{34}S_{CAS}$ (Fig. 2). This periodic enrichment in $\delta^{34}S_{EVAP}$ with respect to $\delta^{34}S_{CAS}$ suggests a relationship between this isotopic offset and changing basin restriction.

ENRICHMENT OF $\delta^{34}S_{EVAP}$

The deposition of each Ara unit (floor anhydrite–carbonate–roof anhydrite) is believed to have taken ~1 m.y. (Bowring et al., 2007); deposition of the floor and roof anhydrites is likely to have taken significantly less time. As such, minimal secular variability in $\delta^{34}S_{SW}$ could have occurred during the deposition of each Ara anhydrite unit (Kah et al., 2004). Further, any such (global) variability is unlikely to oscillate with the same frequency as local (basinal) lithologic changes (e.g., anhydrite-carbonate). Thus, the observed enrichment in $\delta^{34}S_{AN}$ bounding each of the Ara carbonate units must result from a local effect rather than reflect changing $\delta^{34}S_{SW}$.

During abiotic evaporite precipitation, the initial anhydrite and/or gypsum formed is enriched by 1.6‰ relative to seawater sulfate (Raab and Spiro, 1991). The enrichment of ^{34}S in the mineral phase causes the residual sulfate reservoir to be correspondingly ^{34}S depleted. As such, the brine (and thus, coeval evaporites) becomes progressively depleted as evaporation continues (Fig. 4A), according to the standard distillation relationship (Canfield, 2001):

$$\left(^{34}S/^{32}S\right)_{brine} = \left(^{34}S/^{32}S\right)_{SW} \times F^{(\alpha-1)}, \quad (1)$$

where F is the fraction of initial sulfate left in the reservoir and $\alpha = 1.0016$ is the fractionation between coeval gypsum and aqueous sulfate (Raab and Spiro, 1991). The evolution of $\delta^{34}S$ as a function of F necessitates the distinction between bulk and instantaneous $\delta^{34}S$ values. Quantitative removal of sulfate from the brine during evaporite deposition results in average $\delta^{34}S_{EVAP} = \delta^{34}S_{SW}$ (e.g., by integrating the gypsum line in Fig. 4A). However, instantaneous $\delta^{34}S$ values for gypsum range from being enriched with respect to seawater by 1.6‰ to being significantly depleted with respect to seawater as evaporation continues (Fig. 4A). Evaporite deposition at low F may explain reports of evaporites depleted in $\delta^{34}S$ relative to coeval CAS (Kah et al., 2004). An ~1.6‰ enrichment in $\delta^{34}S_{EVAP}$ relative to $\delta^{34}S_{SW}$ (at F ~ 1) is the maximum enrichment that can be attributed to abiotic sulfate (gypsum) precipitation. Substantially larger enrichments (to 4‰ relative to CAS), however, are observed in Ara anhydrites. These enrichments must reflect an additional ^{34}S-depleted sink during evaporite deposition.

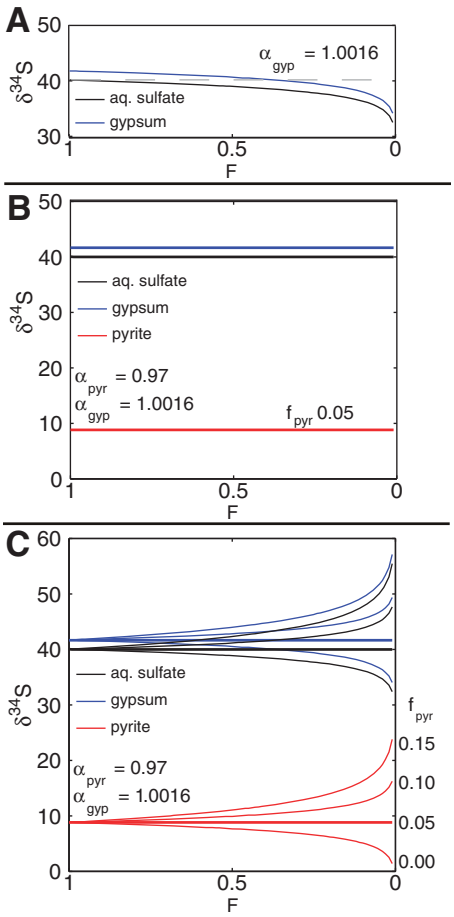

Figure 4. $\delta^{34}S$ evolution as function of F, fraction of sulfate left in reservoir. Initial sulfate reservoir composition is 40‰. A: Aqueous (aq.) sulfate and coeval gypsum (α_{gyp} = 1.0016) decrease in $\delta^{34}S$ as evaporite precipitation progresses. B: Addition of ^{34}S-depleted pyrite sink (α_{pyr} = 0.97) offsets ^{34}S-enriched gypsum sink when pyrite burial, f_{pyr} = 0.05. C: For values of f_{pyr} < 0.05, aqueous and evaporite $\delta^{34}S_{SO_4}$ decrease with sulfate removal, whereas for f_{pyr} > 0.05, $\delta^{34}S_{SO_4}$ increases with sulfate removal. This latter case (f_{pyr} > 0.05) can explain enriched anhydrites of Ara Group.

Bacterial sulfate reduction (BSR) and other microbial metabolisms provide such a sink in most modern sedimentary systems via the biological production of ^{34}S-depleted H_2S (Canfield, 2001). BSR activity is widespread in modern hypersaline systems (Brandt et al., 2001; Habicht and Canfield, 1996; Porter et al., 2007); some of the highest sulfate reduction rates ever recorded occurring in salt marshes and hypersaline microbial mats (Porter et al., 2007). The magnitude of ^{34}S enrichment in the brine depends on isotopic fractionation during BSR and the fraction of sulfate that is reduced to sulfide. Typical fractionations during BSR are 25‰–35‰ with an experimental range of 4‰–46‰ (Canfield and Teske, 1996). Modern hypersaline environments are known to support abundant sulfate reduction characterized by sizeable isotopic fractionations (Fike et al., 2008; Habicht and Canfield, 1996; Habicht and Canfield, 1997). Significant fractionations during BSR are expected to continue throughout evaporite deposition as long as the sulfate reservoir is not drawn sufficiently low (<~200 M) by gypsum precipitation and/or BSR so as to inhibit biological fractionation (Habicht et al., 2002). Fluid inclusion analysis, however, indicates that sulfate remained sufficiently abundant throughout deposition of the Ara anhydrite units to maintain substantial fractionations during BSR (Brennan et al., 2004).

The resulting ^{34}S-depleted sulfide must be sequestered as pyrite (or some other geologically stable reduced sulfur compound) to preserve the isotope enrichment of the brine. While most modern evaporitic environments with high rates of BSR, such as Guerrero Negro (Mexico) and Solar Lake (Egypt), are iron limited, some locations (e.g., Camargue, France) are iron rich (Wieland et al., 2005), and thus have the potential for significant pyrite sequestration. Moreover, it has been proposed that ferruginous conditions were common in both deep and shallow water environments in the Ediacaran-Cambrian ocean (Canfield et al., 2008), most likely due to a shortage of available oxidants. If so, ferruginous conditions could enable efficient capture and sequestration of ambient ^{34}S-depleted H_2S as pyrite during restriction when the Ara basin is cut off from the open ocean. Finely disseminated pyrites occur throughout the Ara anhydrites, particularly along organic-rich lamina (Fig. DR2), as well as in the coeval Al Shomou silicilyte in the basin center (Amthor et al., 2005). As such, we suggest that parallel pyrite sequestration is the most plausible mechanism to generate the enriched $\delta^{34}S_{EVAP}$ observed in Ara Group anhydrites.

The impact of pyrite sequestration on $\delta^{34}S_{EVAP}$ can be evaluated by modifying Equation 1, replacing α with the average fractionation of sulfur leaving the system (α_{avg}):

$$\left(\alpha_{avg}\right) = f_{pyr} \times \left(\alpha_{pyrite}\right) + \left(1 - f_{pyr}\right) \times \left(\alpha_{gypsum}\right), \quad (2)$$

where f_{pyr} is the fraction of sulfur burial due to pyrite formation and $(1 - f_{pyr})$ is the fraction due to sulfate deposition. The modern (globally averaged) marine f_{pyr} is ~0.3 (Canfield, 2001); evaporite deposition is generally assumed to occur with local f_{pyr} ~0, due in part to the rapid deposition of sulfate evaporites (Warren, 1989). From Equation 2, we can calculate the value of f_{pyr} at which the burial of ^{34}S-depleted pyrites balances that of ^{34}S-enriched sulfates (i.e., α_{avg} = 1). For α_{pyrite} = 0.97 (see above) and α_{gypsum} = 1.0016 (Raab and Spiro, 1991), f_{pyr} = 0.05 results in a constant isotopic composition of the brine ($\delta^{34}S_{SW}$) and gypsum (enriched by 1.6‰) as evaporation progresses (Fig. 4B). In this case, there is no difference between instantaneous and average $\delta^{34}S$ for any phase. For f_{pyr} < 0.05, $\delta^{34}S_{brine}$ and $\delta^{34}S_{EVAP}$ decrease as evaporation progresses, and bulk $\delta^{34}S_{EVAP}$ is enriched by <1.6‰ with respect to $\delta^{34}S_{CAS}$. However, for f_{pyr} > 0.05, $\delta^{34}S_{brine}$ and $\delta^{34}S_{EVAP}$ increase with continued evaporation, resulting in bulk $\delta^{34}S_{EVAP}$ enriched by more than 1.6‰ relative to $\delta^{34}S_{CAS}$ (Fig. 4C). In addition, successive evaporites from a single episode would have progressively enriched $\delta^{34}S$ values. We observe that $\delta^{34}S_{EVAP}$ in roof anhydrites often increases from the carbonate-anhydrite to the anhydrite-halite contact, although higher order pulses of freshening or restriction can modulate this signal (Fig. 3). Thus, observing shifts in $\delta^{34}S_{EVAP}$ within first-order evaporative cycles may provide a way to reconstruct pulses of evaporation and freshening during periods of evaporite deposition. Future work pairing high-resolution $\delta^{34}S_{EVAP}$ measurements with the incorporation of trace elements in sulfate evaporites (Kah et al., 2001) can provide constraints on the impact of this effect.

Thus, both the magnitude of the observed enrichment (as much as 4‰ relative to $\delta^{34}S_{CAS}$) in $\delta^{34}S_{AN}$ and the apparent isotope trends within individual Ara anhydrites can be explained as the result of significant bacterial sulfate reduction and pyrite sequestration (f_{pyr} > 0.05) during basin restriction. It is noteworthy that the maximum magnitude of the fractionations is nearly the same (~4‰) in each cycle, suggesting an upper limit to the BSR-induced enrichment effect. Given that all evaporite samples analyzed are bedded anhydrites deposited prior to the onset of halite deposition, we propose that the extent of $\delta^{34}S$ enrichment in the Ara anhydrites is limited by the onset of halite precipitation; this terminates the deposition of continuously bedded sulfates and thereby provides a lower limit on the values of F that can be sampled from within the bedded anhydrites. Analysis of anhydrites within the salt has been avoided because of the high probability of stratigraphic displacement, due to postdepositional halite remobilization.

If we assume that all sulfate was removed from solution and that fractionation during BSR did not change significantly during restriction, we can determine the minimum f_{pyr} necessary to result in a 4‰ enrichment in $\delta^{34}S_{EVAP}$. At f_{pyr} = 0.067 (α_{avg} = 0.9995), the last 1% of sulfate precipitated (i.e., F = 0.01) would have been sufficiently enriched to generate the $\delta^{34}S_{EVAP}$ observed in Ara strata. However, primary fluid inclusions within halite crystals are known to contain abundant residual sulfate (Brennan et al., 2004), indicating that the aqueous sulfate reservoir was not exhausted (F ≫ 0) when the last continuously bedded anhydrites were precipitated.

Therefore, the above estimate of f_{pyr} needed to generate the Ara data is likely to be a significant underestimate. It is possible to estimate F at the termination of calcium sulfate deposition based upon the marine chemistry during Ara deposition as reconstructed by Brennan et al. (2004): Ca^{2+} 14 mmolal and SO_4^{2-} 20.5 mmolal. Given modern dissolved inorganic carbon (DIC) values (~2.4 mmolal), we can approximate F as:

$$F \sim SO_4(f)/SO_4(i) =$$

$$\left[SO_4(i) - (Ca - DIC/2)\right]/SO_4(i) \sim 0.38, \quad (3)$$

(where i is initial and f is final), assuming that calcium removes 50% of the DIC as calcium carbonate and that subsequently sulfate titrates out the remaining calcium (Brennan et al., 2004). This is only an approximation, as some chemical constituents (e.g., DIC) in ancient seawater remain poorly constrained and some residual calcium may have remained in the brine at the time our samples were deposited. For F = 0.38, a value of f_{pyr} ~ 0.13 is needed to generate the observed enrichments in $\delta^{34}S_{EVAP}$ from Ara Group anhydrites (see the Data Repository).

This value for local f_{pyr} (0.13) is substantially higher than generally assumed for evaporite basins, the mineralogy and geochemistry of which generally are thought to be dominated by physical rather than biological processes (Warren, 1989), but only ~15% of estimated global averaged values (0.8) during late Ediacaran–early Cambrian time (Fike and Grotzinger, 2008). We attribute elevated pyrite burial, both globally and locally in association with Ara evaporite deposition, to a general drawdown of oxidants in the marine water column, creating possible ferruginous conditions during late Ediacaran–early Cambrian time (Canfield et al., 2008), which would enable the efficient removal of sulfide as pyrite. If there is a relationship between ferruginous conditions and substantial ^{34}S enrichments in evaporites relative to seawater sulfate, then paired $\delta^{34}S_{CAS}$-$\delta^{34}S_{EVAP}$ data may provide an independent proxy for marine redox through time.

ACKNOWLEDGMENTS

We thank the Oman Ministry of Oil and Gas for permission to publish this paper. This research was supported by Petroleum Development Oman (PDO) and a grant from the Agouron Institute. Fike was also supported by a National Science Foundation Graduate Research Fellowship and the Massachusetts Institute of Technology Global Habitability Longevity Award. We thank PDO for access to samples and logistical support, L. Pratt for use of laboratory facilities and discussions, S. Studley for laboratory assistance, and T. Lyons for comments.

REFERENCES CITED

Amthor, J.E., Grotzinger, J.P., Schroeder, S., and Schreiber, B.C., 2002, Tectonically-driven evaporite-carbonate transitions in a Precambrian/Cambrian saline giant: Ara Salt Basin of south Oman [abs.], *in* AAPG Annual Meeting Proceedings, Houston, Texas: Tulsa, Oklahoma, American Association of Petroleum Geologists, p. A6–A7.

Amthor, J.E., Ramseyer, K., Faulkner, T., and Lucas, P., 2005, Stratigraphy and sedimentology of a chert reservoir at the Precambrian-Cambrian boundary: The Al Shomou Silicilyte, South Oman Salt Basin: GeoArabia, v. 10, p. 89–122.

Bowring, S.A., Grotzinger, J.P., Condon, D.J., Ramezani, J., and Newall, M., 2007, Geochronologic constraints on the chronostratigraphic framework of the Neoproterozoic Huqf Supergroup, Sultanate of Oman: American Journal of Science, v. 307, p. 1097–1145, doi: 10.2475/10.2007.01.

Brandt, K.K., Vester, F., Jensen, A.N., and Ingvorsen, K., 2001, Sulfate reduction dynamics and enumeration of sulfate-reducing bacteria in hypersaline sediments of the Great Salt Lake (Utah, USA): Microbial Ecology, v. 41, p. 1–11.

Brennan, S.T., Lowenstein, T.K., and Horita, J., 2004, Seawater chemistry and the advent of biocalcification: Geology, v. 32, p. 473–476, doi: 10.1130/G20251.1.

Burdett, J.W., Arthur, M.A., and Richardson, M., 1989, A Neogene seawater sulfate isotope age curve from calcareous pelagic microfossils: Earth and Planetary Science Letters, v. 94, p. 189–198, doi: 10.1016/0012-821X(89)90138-6.

Canfield, D.E., 2001, Biogeochemistry of sulfur isotopes: Reviews in Mineralogy and Geochemistry, v. 43, p. 607–636, doi: 10.2138/gsrmg.43.1.607.

Canfield, D.E., and Teske, A., 1996, Late Proterozoic rise in atmospheric oxygen concentration inferred from phylogenetic and sulphur-isotope studies: Nature, v. 382, p. 127–132, doi: 10.1038/382127a0.

Canfield, D.E., Poulton, S.W., Knoll, A.H., Narbonne, G.M., Ross, G.M., Goldberg, T., and Strauss, H., 2008, Ferruginous conditions dominated later Neoproterozoic deep-water chemistry: Science, v. 321, p. 949–952, doi: 10.1126/science.1154499.

Claypool, G.E., Holser, W.T., Kaplan, I.R., Sakai, H., and Zak, I., 1980, The age curves of sulfur and oxygen isotopes in marine sulfate and their mutual interpretation: Chemical Geology, v. 28, p. 199–260, doi: 10.1016/0009-2541(80)90047-9.

Fike, D.A., and Grotzinger, J.P., 2008, A paired sulfate-pyrite $\delta^{34}S$ approach to understanding the evolution of the Ediacaran-Cambrian sulfur cycle: Geochimica et Cosmochimica Acta, v. 72, p. 2636–2648, doi: 10.1016/j.gca.2008.03.021.

Fike, D.A., Grotzinger, J.P., Pratt, L.M., and Summons, R.E., 2006, Oxidation of the Ediacaran ocean: Nature, v. 444, p. 744–747, doi: 10.1038/nature05345.

Fike, D.A., Gammon, C.L., Ziebis, W., and Orphan, V.J., 2008, Micron-scale mapping of sulfur cycling across the oxycline of a cyanobacterial mat: A paired nanoSIMS and CARD-FISH approach: ISME Journal, v. 2, p. 749–759, doi: 10.1038/ismej.2008.39.

Garrels, R.M., and Lerman, A., 1981, Phanerozoic cycles of sedimentary carbon and sulfur: National Academy of Sciences Proceedings, v. 78, p. 4652–4656.

Habicht, K.S., and Canfield, D.E., 1996, Sulphur isotope fractionation in modern microbial mats and the evolution of the sulphur cycle: Nature, v. 382, p. 342–343.

Habicht, K.S., and Canfield, D.E., 1997, Sulfur isotope fractionation during bacterial sulfate reduction in organic-rich sediments: Geochimica et Cosmochimica Acta, v. 61, p. 5351–5361, doi: 10.1016/S0016-7037(97)00311-6.

Habicht, K.S., Gade, M., Thamdrup, B., Berg, P., and Canfield, D.E., 2002, Calibration of sulfate levels in the Archean Ocean: Science, v. 298, p. 2372–2374, doi: 10.1126/science.1078265.

Kah, L.C., Lyons, T.W., and Chesley, J.T., 2001, Geochemistry of a 1.2 Ga carbonate-evaporite succession, northern Baffin and Bylot Islands: Implications for Mesoproterozoic marine evolution: Precambrian Research, v. 111, p. 203–234, doi: 10.1016/S0301-9268(01)00161-9.

Kah, L.C., Lyons, T.W., and Frank, T.D., 2004, Low marine sulphate and protracted oxygenation of the Proterozoic biosphere: Nature, v. 431, p. 834–838, doi: 10.1038/nature02974.

Kampschulte, A., and Strauss, H., 2004, The sulfur isotopic evolution of Phanerozoic seawater based on the analysis of structurally substituted sulfate in carbonates: Chemical Geology, v. 204, p. 255–286, doi: 10.1016/j.chemgeo.2003.11.013.

Lyons, T.W., Walter, L.M., Gellatly, A.M., Martini, A.M., and Blake, R.E., 2004, Sites of anomalous organic remineralization in the carbonate sediments of south Florida, USA; the sulfur cycle and carbonate-associated sulfate, *in* Amend, J.P., et al., eds., Sulfur biogeochemistry: Past and present: Geological Society of America Special Paper 379, p. 161–176.

Porter, D., Roychoudhury, A.N., and Cowan, D., 2007, Dissimilatory sulfate reduction in hypersaline coastal pans: Activity across a salinity gradient: Geochimica et Cosmochimica Acta, v. 71, p. 5102–5116, doi: 10.1016/j.gca.2007.08.023.

Raab, M., and Spiro, B., 1991, Sulfur isotopic variations during seawater evaporation with fractional crystallization: Chemical Geology, v. 86, p. 323–333.

Schröder, S., Schreiber, B.C., Amthor, J.E., and Matter, A., 2003, A depositional model for the terminal Neoproterozoic–Early Cambrian Ara Group evaporites in south Oman: Sedimentology, v. 50, p. 879–898, doi: 10.1046/j.1365-3091.2003.00587.x.

Schröder, S., Schreiber, B.C., Amthor, J.E., and Matter, A., 2004, Stratigraphy and environmental conditions of the terminal Neoproterozoic-Cambrian period in Oman: Evidence from sulphur isotopes: Geological Society of London Journal, v. 161, p. 489–499.

Warren, J.K., 1989, Evaporite sedimentology: Importance in hydrocarbon accumulation: Englewood Cliffs, New Jersey, Prentice Hall, 285 p.

Wieland, A., Zopfi, J., Benthien, A., and Kuhl, M., 2005, Biogeochemistry of an iron-rich hypersaline microbial mat (Camargue, France): Microbial Ecology, v. 49, p. 34–49, doi: 10.1007/s00248-003-2033-4.

Worden, R.H., Smalley, P.C., and Fallick, A.E., 1997, Sulfur cycle in buried evaporites: Geology, v. 25, p. 643–646, doi: 10.1130/0091-7613(1997)025<0643:SCIBE>2.3.CO;2.

Manuscript received 12 March 2009
Revised manuscript received 9 November 2009
Manuscript accepted 10 November 2009

Printed in USA